JMEPEG (2023) 32:211–220
https://doi.org/10.1007/s11665-022-07096-6

1059-9495/$19.00

TECHNICAL ARTICLE

Producing Nanobainite on Carburized Surface of a Low-Carbon Low-Alloy Steel

Behzad Avishan, Peyman Talebi, Süleyman Tekeli, and Sasan Yazdani

Submitted: 21 February 2022 / Revised: 30 April 2022 / Accepted: 20 May 2022 / Published online: 5 July 2022

Conducting the carburizing process on the surface layer of low-carbon steel and subsequent austempering heat treatment can be implemented to obtain nanobainite microstructure on the surface of steels. In this research, steel with 0.23 wt.% carbon was carburized for 3 h at 900 °C in a liquid salt bath containing sodium cyanide, sodium carbonate, and sodium chloride and immediately quenched to room temperature. The samples were then heated to 900 °C for 30 min and isothermally transformed at three different temperatures of 200, 250 and 300 °C for 72, 24 and 12 h, respectively. It was found that nanostructured bainite was formed on the surface layer and the subunits of bainitic ferrite and high-carbon austenite films were almost 60-300 nm thick depending on the heat treatment temperature. It was also found that the samples austempered at these temperatures contained 18, 21 and 28% volume fractions of retained austenite on the surfaces, respectively. Due to the comparable microstructural characteristics, similar friction coefficients were obtained as for ordinary nanostructured bulk bainitic steels with high-carbon content.

Keywords carburizing, electron microscopy, heat treatment, nanostructured Bainite, optical microscopy, steel, x-ray diffraction

1. Introduction

Nanostructured bainitic steels (NBS), as a new category of advanced carbide-free bainitic steels (CFB), are desirable engineering materials for producing of high-performance steels due to their exceptional strength-ductility properties compared to many advanced high-strength iron-based alloys. While the ordinary bainite microstructure contains bainitic ferrite with a thickness of nearly 0.2-0.5 μm and a length of 100 μm (Ref 1), bainitic subunits thinner than 100 nm can be successfully attained in NBS after isothermal austempering heat treatment in the temperature range of 200-400 °C, separated with austenite films of similar thickness in each bainitic sheaf, and the resultant microstructural features confirm the improved mechanical properties, which are comparable to many advanced high-strength steels (Ref 2-9). The size and volume fraction of the microstructural constituents depend on the heat treatment temperature so that finer microstructural features and higher volume fractions of bainitic sheaves can be obtained at lower heat treatment temperatures. The key point is that the production method involves only a simple heat treatment of a bulk material and does not require a complicated production process (Ref 10).

The conventional chemical composition for the production of a nanostructured bainitic steel is 0.6-1.0 C, 1.5-2 Si, 0.7-2 Mn and 0.4-1.7 Cr (all in wt.%), which makes it possible to carry out the isothermal bainitic heat treatment at very low temperatures because of the low martensite start (Ms) and bainite start (Bs) temperatures. Moreover, the formation of any diffusional phase transformation products is prohibited due to the sufficiently high hardenability of the steel (Ref 11). Despite the fact that a high-carbon content is necessary for the production of nanostructured bainite, the weldability limitations have led researchers to find different methods to produce NBS in steel with a lower amount of carbon without deterioration of the final strength and ductility combination (Ref 12). Consequently, multistep austempering (Ref 13, 14), ausforming of the primary steel before implementing the austempering heat treatment (Ref 15, 16), and carburizing the surface layer of low-carbon steel (Ref 11) were proposed as successive approaches.

Among those, carburizing and subsequent austempering heat treatment procedure has received considerable attention in the production of NBS, especially when high wear resistance on the surface of the material is of great importance. The considerable wear resistance of nanobainite microstructure in Fe-based alloys has been previously confirmed (Ref 17, 18) and attributed to the unique microstructural characteristics and transformation-induced plasticity (TRIP) effect for which the volume fraction and morphology of austenite and its stability are of great importance. In this regard, the carburizing + austempering process would allow to benefit from carbon reduction and achieving high wear performance simultaneously. Yang and Zhang (Ref 19) showed that low-carbon steels with the chemical composition of 0.18-0.35 C, 0.32-1.54 Si, 0.0-1.77 Mn, 1.31-1.72 Cr, 0.018-0.38 Mo, 0.0-1.35 Al, 0.0-2.3 Ni, and 0.0.16 Cu (in wt.%) are suitable to obtain nanostruc-

Behzad Avishan, Department of Materials Engineering, Azarbaijan Shahid Madani University, P.O.Box: 53714-161, Tabriz, Iran; **Peyman Talebi** and **Sasan Yazdani**, Faculty of Materials Engineering, Sahand University of Technology, Tabriz, Iran; and **Süleyman Tekeli**, Department of Metallurgical and Materials Engineering, Faculty of Technology, Gazi University, Ankara, Turkey. Contact e-mails: avishan@azaruniv.ac.ir yazdani@sut.ac.ir.

tured bainite after carburizing process. Hayrynen et al. (Ref 20) demonstrated that carburizing at 850-950 °C and immediately quenching to a temperature just above the M_s of the steel to complete the bainite transformation, or immediate cooling to room temperature after carburizing at the same temperature range, reheating the carburized sample to 850-950 °C and quenching to a temperature above the M_s and conducting the austempering isothermal heat treatment, both can successfully result in steels with nanostructured bainite at the surface layer and low-carbon martensite at the center. Diez et al. (Ref 21) have shown that the carbo-austempering process can lead to considerable wear resistance in steels, which is even better than that of a quenched and tempered microstructure, considering the desired microstructural characteristics, hardening behavior and plasticity of the material.

Given the importance of carbon element for providing the necessary thermodynamic conditions for nanobainite formation and the importance of the reduction of carbon content to improve the weldability, makes it vital to investigate carburizing heat treatment and consequent austempering process as an effective production process for obtaining NBS. This article aims to study the microstructural characteristics at the surface layer of steel with 0.23 wt.% carbon after carburizing + austempering heat treatments at different isothermal bainite transformation temperatures. Furthermore, the wear resistance of the materials was compared with that of conventional nanostructured bulk bainitic steels with high-carbon content to determine whether carburizing and consequent austempering can produce wear behavior similar to that of these high-carbon steels with nanostructured bainite in their microstructure.

2. Materials and Methods

The chemical composition of the primary steel was designed based on the thermodynamic theories of bainite transformation using the MUCG83™ thermodynamic model (Ref 22) and the low-carbon steel was cast in an induction furnace. Electro-slag remelting (ESR) was carried out to eliminate the inclusions as much as possible and to obtain clean steel with the final chemical composition given in Table 1. The primary steel was homogenized at 1200 °C for 4 h and hot rolled into 15 mm thick plates in several passes with a thickness reduction of 25% in each pass. The steel sheet was machined on both sides to cut out the decarburized layers. Test samples were then cut from the sheet using an electric discharge machine to perform the carburizing and austempering heat treatment process (see Fig. 1). The samples were carburized in a molten salt furnace with a composition of 40% sodium cyanide + 40% sodium carbonate + 20% sodium chloride at 900 °C for 3 h and immediately cooled to room temperature at the end of the carburizing process. The chemical composition of the carburized layer on the surface of the material was determined by quantometer analysis, and it was found that the carbon content on the carburized surface increased to almost 0.8 wt.% (see Table 1). Carburized specimens were cross-sectioned and the thickness of the carburized layer was determined using the microhardness test profile. Microhardness tests were performed from the surface to the center of the material with a load of 200 g using a Germanischer M400-G1™ instrument.

Carburizing heat treatment was followed by reheating the samples to 900 °C holding for 30 min and austempering at 300, 250 and 200 °C for 12, 24 and 72 h, respectively, to produce nanostructured bainite on the steel surface. Both austenitizing and austempering heat treatments were conducted in salt bath furnaces. Primary microstructural evaluations of the carburized and austempered samples were performed using an Olympus PMG3™ optical microscope (OM) after grinding, polishing, and etching with 2% Nital etching solution. Furthermore, three-step etching with Nital + picral + sodium metabisulfite etching solutions was used when it was necessary to evaluate the formation of the martensite phase in the inner layers. More detailed microstructural studies were performed using a Mira3 Tescan™ field emission scanning electron microscope (FE-SEM) at high magnifications to determine the thickness of the bainitic ferrite and austenite film phases within the bainitic sheaves. Thicknesses were determined by at least 10 measurements in at least 10 high magnification images using the line intercept method (Ref 23). The mean values of the thicknesses of the bainitic ferrite and austenite films were reported in each case with calculated standard deviations. The distribution of austenite blocks was analyzed using the IMAGE J™ image analysis program based on the OM micrographs. The hardness of the carburized surface was determined using an EseWay™

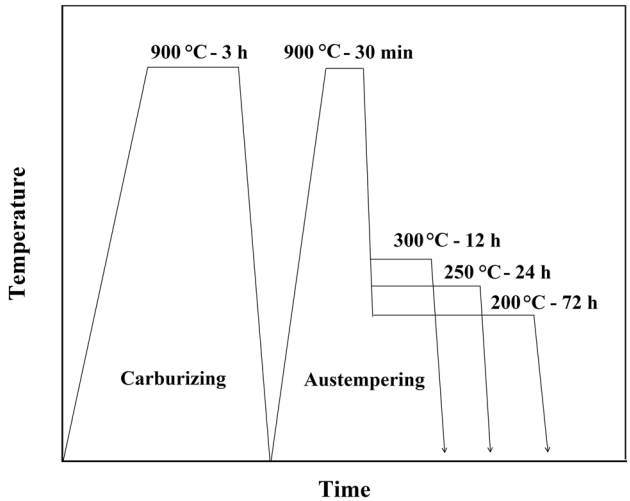

Fig. 1 Carburizing and consequent austempering process applied to steel

Table 1 The chemical composition of the primary steel and the chemical composition on the carburized surface layer

Alloying element	C	Si	Mn	Cr	Mo	Ni	Cu	V
Chemical composition of the Raw material	0.23	1.33	0.90	1.11	0.23	3.24	0.96	0.11
Chemical composition of the surface after carburizing	0.80	1.33	0.90	1.11	0.22	3.12	0.92	0.10

machine in the HV30 scale and the average of at least 4 measurements was reported.

X-ray diffraction (XRD) was used to determine the volume fraction of the high-carbon retained austenite on the surface of the carburized and austempered steels at the end of the different heat treatment processes. In addition, the carbon content of the retained austenite was calculated using the method described by Dyson and Holmes (Ref 24). The XRD investigations were performed using a Bruker-Axs D8 Advance™ x-ray diffractometer with monochromated CuKα radiation in a 2θ range of 40 - 105° with a scanning speed of 3 seconds at a scanning step of 0.03°. The volume fraction of austenite was determined from the integrated intensities of the (200), (220) and (311) peaks of austenite and the (200), (211) and (220) peaks of ferrite (Ref 25).

Pin-on-disk wear tests were performed on carburized and annealed specimens using ASTM G99 standard procedure to compare the wear resistance of the materials with that of previously reported for ordinary nanostructured bulk bainitic high-carbon steels. In addition, the wear performance of the specimens was compared with that of carburized and quenched specimens without implementing the austempering heat treatment. The grinding wheel for the wear tests was a 13 cm diameter AISI 52100 bearing steel that was austenitized at 850 °C for 45 minutes, quenched in oil, and finally tempered at 150 °C for 30 minutes. The hardness of the grinding wheel was 800 HV30, and the tests were performed at a load of 40 N and a wear distance of 2000 m with a sliding speed of 0.3 ms^{-1}. At least 2 wear tests were performed under each condition, and the friction coefficients were reported as a primary criterion for evaluating the wear performance.

3. Results and Discussion

The profile of the microhardness test from the surface to the center of the carburized steel before the austempering heat treatment shown in Fig. 2 indicating that the thickness of the carburized layer was nearly 1.7 mm. Figure 3 depicts the

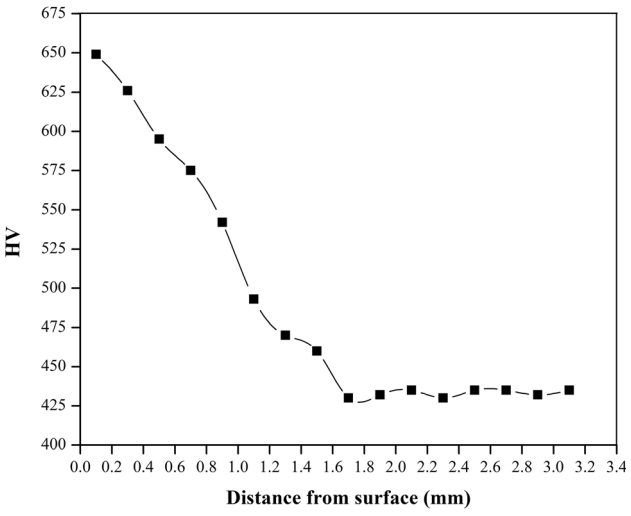

Fig. 2 Microhardness test profile from the surface to the center of the carburized steel before performing reheating and austempering heat treatment to determine the thickness of the carburized layer

microstructural characteristics of the carburized and austempered samples at the end of the isothermal bainite transformations at 300, 250 and 200 °C. The images were taken from the cross sections of the heat-treated samples at 100 μm from the surface. It is evident that carburization and subsequent austempering heat treatment resulted in bainitic sheaves being separated by austenite micro-blocks on the surface of the steel. Additionally, it can be seen that a decrease in the austempering temperature resulted in a higher volume fraction of bainitic sheaves finer in size which can be justified by the different driving force of bainite transformation at different austempering temperatures. Bainite transformation starts with the paraequilibrium nucleation of bainitic ferrite from the primary austenite grain boundaries and progresses by its shear growth (Ref 1). A reduction in bainite transformation temperature increases the driving force of the bainite reaction so that a higher volume fraction of bainitic ferrite can be achieved. On the other hand, a higher volume fraction of bainite formation results in more severe impingement of the sheaves, which limits their further growth. As a result, finer bainitic sheaves with higher volume fraction can be obtained if the austempering temperature is lower.

The formation of a higher bainite volume fraction directly affects the volume fraction and size of austenite micro-blocks in the microstructure of the specimens. Higher amount of bainite formation consumes more primary austenite and consequently reduces the size and volume fraction of the final austenite blocks. This can be easily followed in the images of OM in Fig. 4, where the bainitic sheaves and austenite blocks are marked with blue and red colors, respectively. It is clear that lowering the austempering temperature from 300 to 200 °C results in a decreased amount of austenite blocks with smaller mean diameters.

Knowing that the carbon content changes from the carburized surface toward the center of the steel, it is logical that different volume fractions of bainite and austenite will form at different locations, and martensite is expected to form at interior surfaces with lower carbon content. This is because the hardenability at different points of the carburized material changes from the surface to the inner layers because the carbon content is lower at inside layers. Theoretical calculations using the MUCG83™ thermodynamic model showed that the M_s temperature at the carburized surface of the material with 0.8 wt.% carbon was nearly 55 °C, while it increased with increasing distance from the carburized surface to the center of the material, and the M_s temperature of the center regions with 0.23 wt.% carbon was estimated to be nearly 310 °C. Obviously, the increase in M_s temperature in the inner layers below the carburized surface causes the retained austenite to transform into martensite, the volume fraction of which becomes higher with increasing depth from the surface layer. Accordingly, while bainite and high-carbon retained austenite were present at the surface of the carburized and austempered materials, they were partially replaced by martensite in the layers below the surface. Figure 5 shows examples of the OM images from the layers well below the carburized surface of the samples that were austempered at each bainite transformation temperature and it can be seen that the martensite phase could be identified in brown colors alongside bainitic sheaves and austenite micro-blocks.

Optical images were not able to distinguish the bainitic ferrite and austenite film within the bainitic sheaves. Therefore, FE-SEM images were used to determine the extent of these

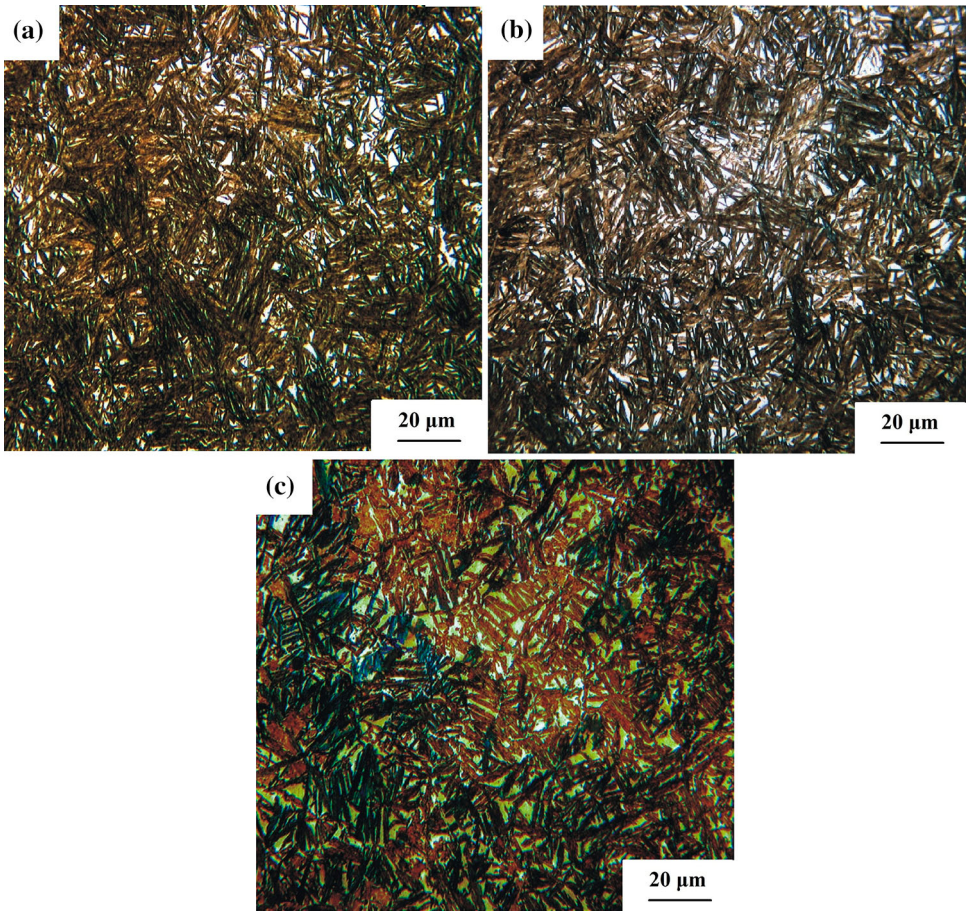

Fig. 3 OM images of the carburized and austempered samples after isothermal bainite transformation at (a) 200 °C/72 h, (b) 250 °C/24 h and (c) 300 °C/12 h

microstructural constituents, which are shown at various magnifications in Fig. 6. It has been shown that bainitic subunits and austenite films with different thicknesses could be obtained after carburizing and austempering at various austempering temperatures, results of which are summarized in Table 2.

Several parameters contribute to the final thickness of bainitic ferrite and austenite film in NBS. Of all the parameters, the strength of the primary austenite has the most significant effect that must be considered when discussing the size of the microstructural features (Ref 26). Higher strength of primary austenite at lower transformation temperatures restricts the motion of the glissile interface between austenite and ferrite, allowing thinner bainitic subunits to be achieved. This is the reason why bainitic subunits and austenite films are thicker in materials austempered at higher temperatures due to the lower strength of the austenite surrounding the bainitic subunits during bainite transformation. On the other hand, the dislocations in the bainitic ferrite and the austenite interfaces generated by the shear nature of the bainite transformation further restrict the growth of the bainitic subunits into the austenite and this is more pronounced when higher density of dislocations is present. At lower transformation temperatures, more dislocations are generated in the microstructure because of the stronger austenite and its more severe strain hardening that in turn further hinders the growth of the bainitic subunits (Ref 27, 28). It has been shown that the dislocation densities for NBS with similar chemical composition of the carburized surface of this study were nearly 3-5 $\times$ 10^{15}, 6-8 $\times$ 10^{15} and 6-9 $\times$ 10^{15} m^{-2} after austempering at 300, 250 and 200 °C, respectively (Ref 29). Thus, a similar trend is expected for carburized and austempered steels and the higher dislocation density at lower transformation temperature justify the finer bainitic subunit formation. Finally, the nucleation rate of bainitic subunits and their interactions during growth must be considered as another important factor determining the thickness at different transformation temperatures. At lower transformation temperatures, a higher driving force of bainitic transformation leads to more bainite formation and more severe impingement of sheaves further restricts their growth, eventually leading to a finer microstructure. Since the thickness of austenite films directly depends on the size of bainitic subunits, thinner austenite films

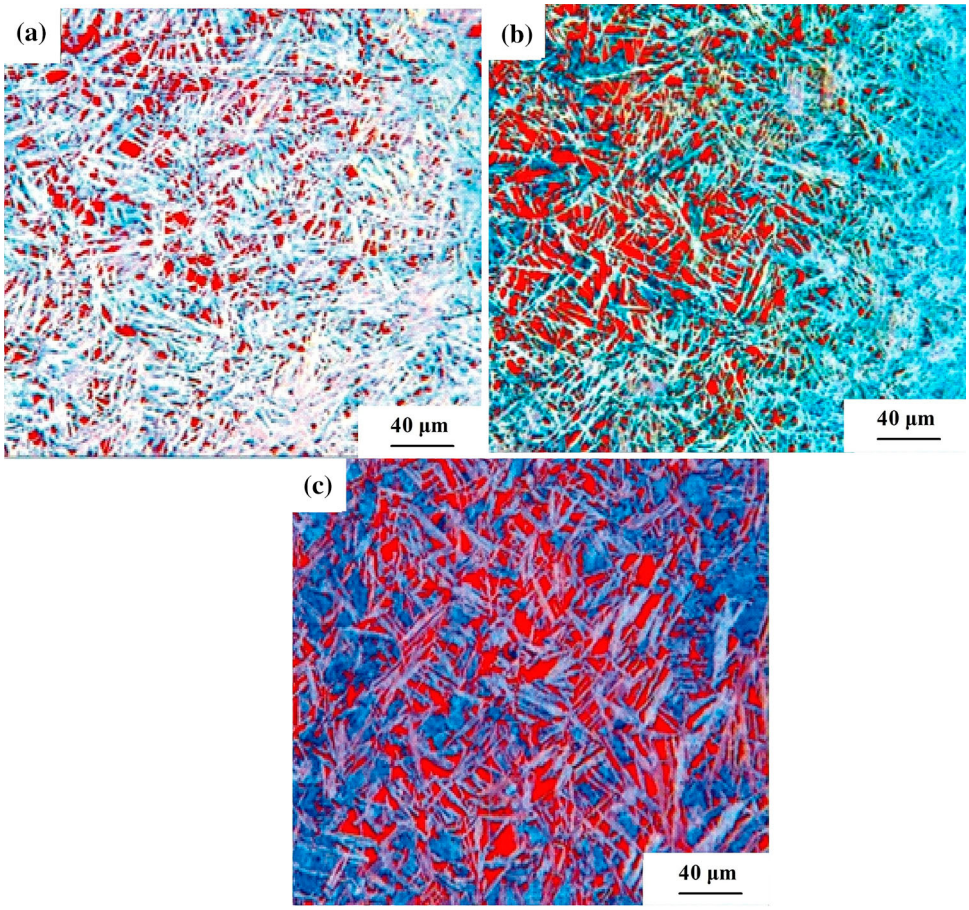

Fig. 4 Bainitic sheaves in blue and austenite micro-blocks in red colors in carburized and austempered samples after isothermal bainite transformation at (a) 200 °C/72 h, (b) 250 °C/24 h and (c) 300 °C/12 h (Color figure online)

would be obtained if the bainitic subunits are thinner (Ref 23). Bainite formation progresses until the carbon content of the surrounding austenite reaches the value predicted by the T_o diagram, i.e., the locus of the points where ferrite and austenite have the same free energies (Ref 30-32). In thicker bainitic ferrite, the carbon partitioning takes place at greater distances in front of the ferrite/austenite interface, so that thicker austenite films can be obtained.

The volume fraction and thickness of the bainitic subunits are the most important factors determining the hardness of the NBS. Obviously, a higher volume fraction of thinner bainitic subunits would increase the hardness value in carburized and austempered steels. This is consistent with the results of this study (see Table 2). It was shown that the hardness values were 492±10, 522±10 and 558±10 HV30 at the carburized surfaces of the steels after austempering at 300, 250 and 200 °C, respectively.

It was mentioned that the high-carbon retained austenite in NBS is present in two filmy and blocky morphologies and its volume fraction depends on the volume fraction of bainite formed in the microstructure. XRD studies of carburized and austempered surfaces can be found in Fig. 7, showing the ferrite and austenite peaks. The results of the refinements of the XRD profiles are summarized in detail in Table 2. Refinement of the XRD profiles indicates that 18, 21, and 28% high-carbon retained austenite formed on the surface of the carburized steels after the austempering heat treatment at 200, 250 and 300 °C, respectively (see Table 2). It is evident that the formation of higher amount of bainite at lower transformation temperatures resulted in more consumption of austenite and consequently a lower volume fraction of austenite remained in the microstructure.

The assumption is that the remaining austenite in samples annealed at lower transformation temperatures must be more carbon enriched because of the higher amount of bainitic ferrite formation and more considerable carbon partitioning to the surrounding austenite. However, the results were in contradiction with theory, as it can be seen in Table 2, which shows that a decrease in austempering temperature after carburizing resulted in a decrease in the carbon content of the solid solution in the austenite phase. This can be attributed primarily to the influence of stress on the lattice parameter of the austenite phase that has

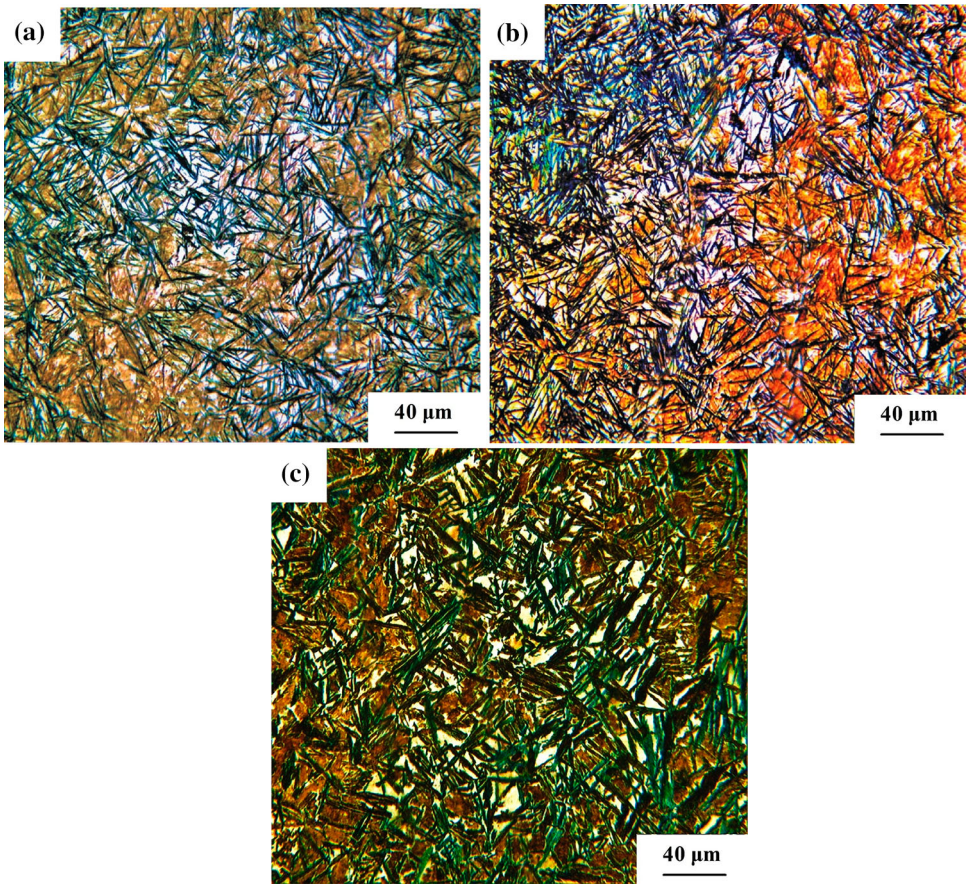

Fig. 5 OM Images of internal layers below the carburized surfaces in carburized and austempered samples after isothermal bainite transformation at (a) 200 °C/72 h, (b) 250 °C/24 h and (c) 300 °C/12 h

been obtained from the positions of the diffraction peaks in the XRD profile. Due to the shear mechanism of bainite transformation, the formation of the bainitic subunit generates compressive stresses in the surrounding austenite phase, which cause a decrease in the lattice parameter and lead to a shift of the austenite peaks in the opposite way than the influence of carbon enrichment. Therefore, it is logical to assume that the calculated carbon concentration will lead to lower values at lower austempering temperatures, where the compressive stresses are more pronounced. On the other hand, the presence of dislocations at the interface between the bainitic subunits and the austenite films must also contribute to underestimation of the carbon content. The dislocation density at the interface between the austenite and bainitic ferrite phases limits the complete carbon depletion from the ferrite into the austenite, and the carbon atoms become trapped in the dislocations. This becomes even more evident when the austempering transformation temperature is lower, as more dislocations are introduced into the microstructure. Finally, the effect of transformation temperature on the long-distance partitioning of carbon atoms should not be ignored when considering the carbon content of the remaining austenite in the microstructure of the NBS. At a lower transformation temperature, the carbon partitioning is not as severe as that of higher austempering temperature, which could lead to a decrease in carbon in solid solution in the surrounding austenite. However, the austenite blocks surrounding the bainitic sheaves are so small that they are still thermally stable at room temperature.

While the volume fraction and thickness of the bainitic ferrite are the most important factors in the hardness and strength properties of NBS, the volume fraction and morphology of the high-carbon retained austenite in the microstructure control the ductility properties. However, the positive role of the austenite phase on strength and hardness cannot be ignored when considering the TRIP effect that occurs when the sample is strained. An effective TRIP effect can simultaneously improve the strength and ductility of NBS. Therefore, it is essential to replace the mechanically less stable blocky austenite with austenite films which are more stable.

It has been shown that nanobainite can be achieved on the surface of low-carbon steels after the application of the carburizing + austempering heat treatment process with

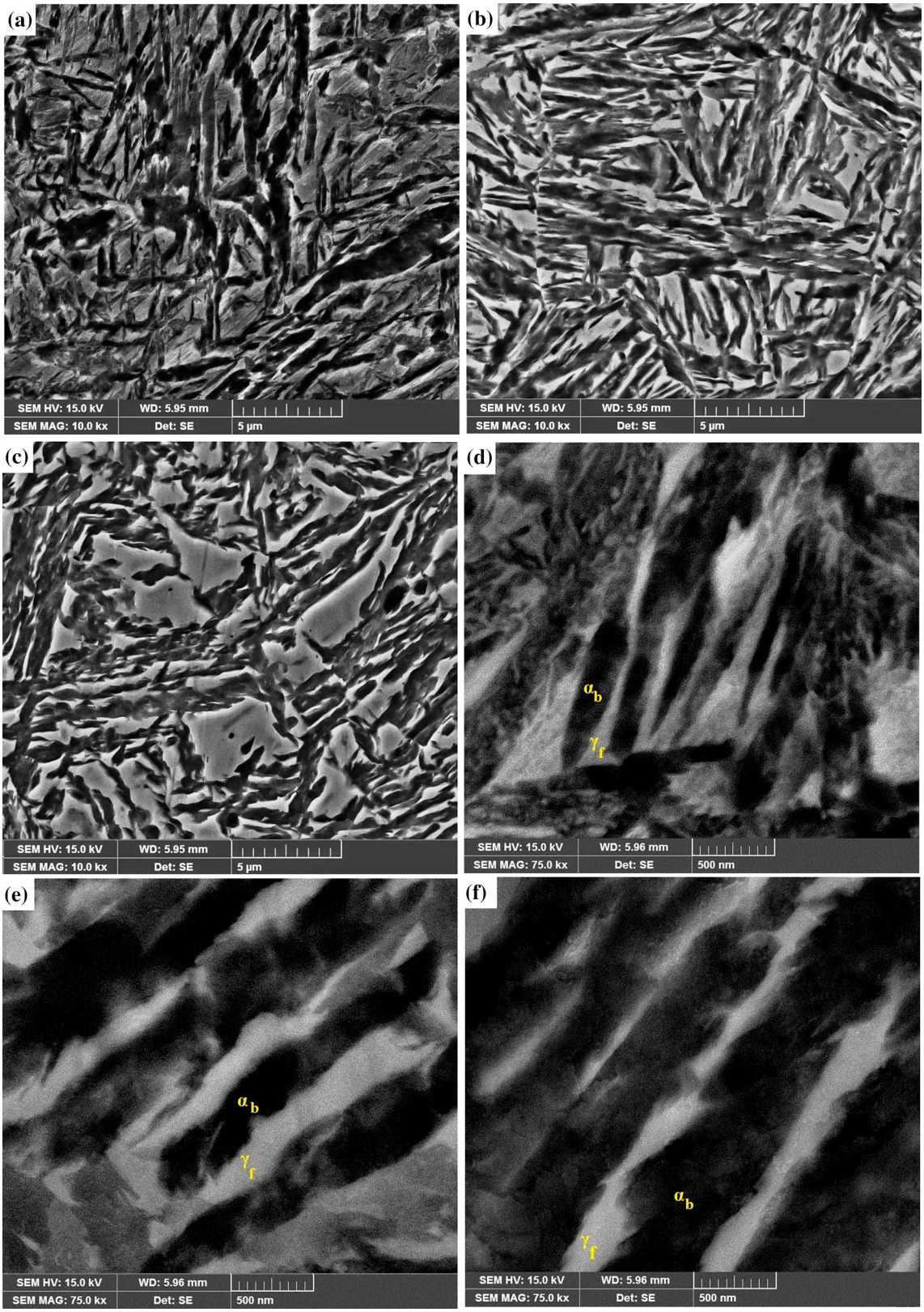

Fig. 6 FE-SEM images of the carburized and austempered samples after isothermal bainite transformation at a and (d) 200 °C/72 h, (b) and (e) 250 °C/24 h and c and (f) 300 °C/12 h

Table 2 Thickness of bainitic subunit ($t_{\alpha b}$) and austenite film ($t_{\gamma f}$), hardness (HV30), volume fraction of austenite (V_γ) and austenite carbon content (C_γ) in heat-treated steels

Austempering temperature/ temperature	$t_{\alpha b}$	$t_{\gamma f}$	HV30	V_γ	C_γ
300 °C/12 h	290±3 nm	160±3 nm	492±10	28%	1.18
250 °C/24 h	150±4 nm	100±4 nm	522±10	21%	1.01
200 °C/72 h	68±3 nm	55±3 nm	558±10	18%	0.94

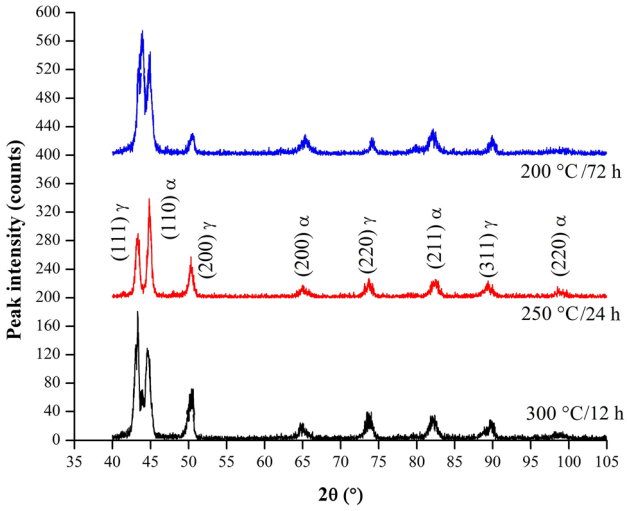

Fig. 7 XRD profiles from the surface of the carburized and austempered samples

microstructural features similar to those of ordinary high-carbon bulk NBS. Accordingly, comparable wear behavior can also be expected. Therefore, the friction coefficients obtained from the pin-on-disk wear tests were used as a first step to support this idea. The results are shown in Fig. 8. The coefficients of friction given in the wear profiles are average values obtained after 2000 m of sliding distance. A higher value means a stronger contact between the surfaces and a higher wear intensity. The results indicate that isothermal bainite transformation in carburized steel results in better wear performance compared to carburized and quenched material, and that samples austempered at a lower transformation temperature have better wear resistance. Friction coefficient values for carburized and austempered steels were in good agreement with those previously reported (μ= 0.5-0.6) for high-carbon bulk NBS obtained after austempering in the temperature range of 200-300 °C and whose chemical composition was comparable to that at the surface of the materials in this study (Ref 33, 34). This suggests that the nanostructured bainite formed at the surface of the original low-carbon steel after carburizing and austempering makes the material suitable for using in industrial applications when wear resistance at the surface is the main requirement, rather than using a high-carbon bulk NBS. However, the coefficient of friction cannot be used alone to confirm this idea. Further detailed investigation and determination of the effective wear performance parameters are mandatory which was not the primary objective of this study, but related researches are in progress for more precise evaluations.

4. Conclusions

Carburization of the primary steel with a carbon content of 0.23 wt.% and subsequent austempering heat treatment at temperatures of 300, 250 and 200 °C resulted in a nanostructured bainite microstructure at the surface, consisting of bainitic subunits and austenite films less than 290 nm thick. The microstructural features were identical to those of bulk nanostructured high-carbon steels and the martensite phase was shown to be formed in the inner layers due to the lower carbon content diffusing from the carburized surface of the material to deeper regions. Bainitic sheaves were separated by austenite micro-blocks, the volume fraction and size of which depended on the austempering temperature. Nanoscale bainitic ferrite formation on the carburized and austempered surface layers resulted in hardness values of 492, 522 and 558 HV30 after isothermal bainitic transformation at 300, 250 and 200 °C, respectively, which were similar to those of bulk nanostructured bainitic steels with high-carbon content. The austempering temperature affected the volume fraction of the high-carbon retained austenite on the carburized surface and the maximum volume fraction of austenite was obtained at the end of the highest austempering temperature. The friction coefficients,

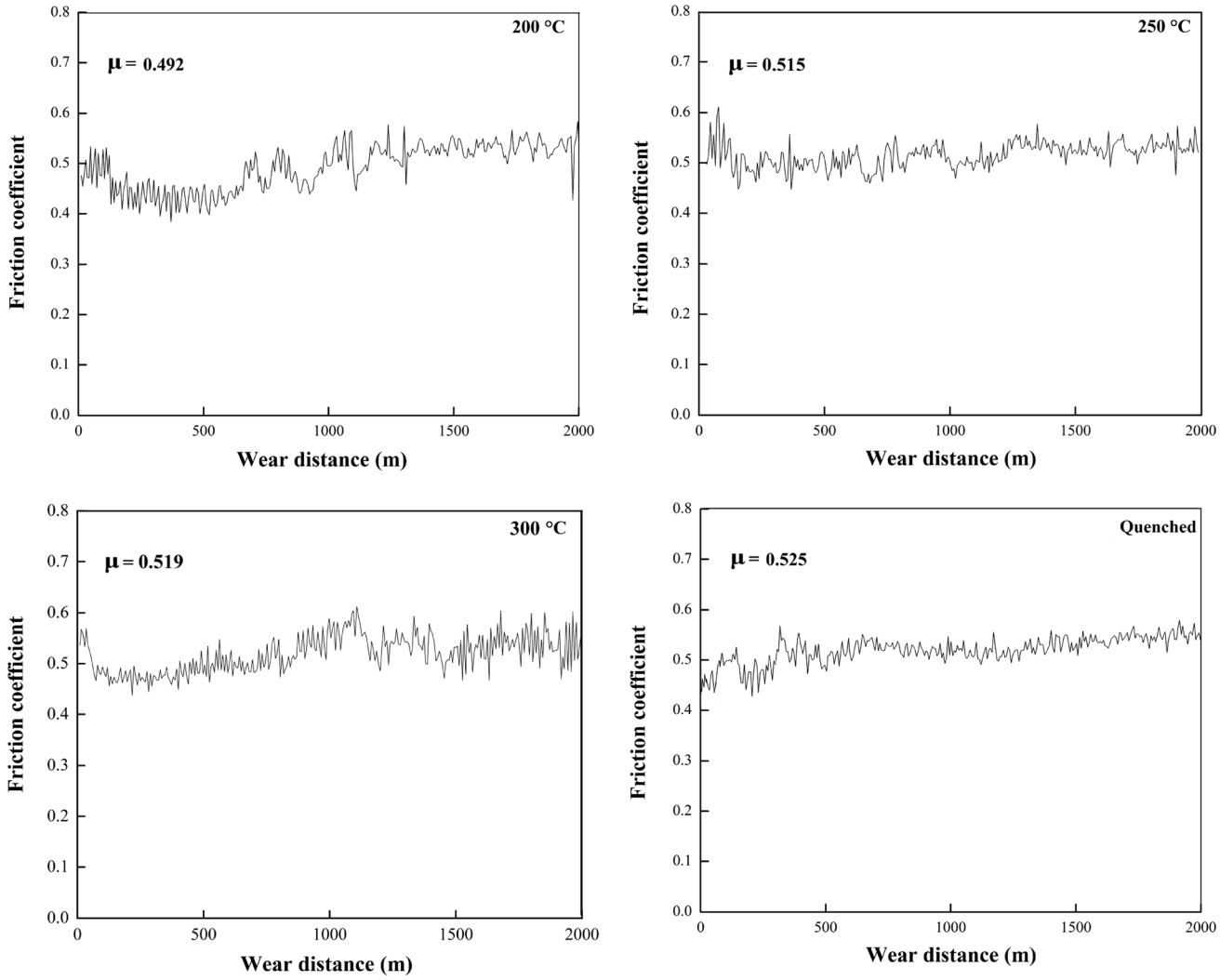

Fig. 8 Friction coefficient (μ) obtained from wear tests for carburized and austempered samples after isothermal bainite transformation at 200 °C/72 h, 250 °C/24 h and 300 °C/12 h compared to quenched sample

obtained from the pin-on-disk wear tests for the carburized and austempered specimens, were in good agreement with the values previously reported for ordinary high-carbon nanostructured bainitic steels. This suggests that the nanostructured bainite formed on the surface of the original low-carbon steel after carburizing and austempering makes the material suitable for use in industrial applications when surface wear resistance is the main requirement, rather than using a high-carbon bulk NBS.

Acknowledgments

The authors are grateful to Sahand University of Technology for providing the research facilities.

References

1. H.K.D.H. Bhadeshia, *Bainite in Steels*, 2nd ed. Institute of Materials, London, 2001
2. C. García Mateo, F.G. Caballero, and H.K.D.H. Bhadeshia, Development of Hard Bainite, *ISIJ Int.*, 2003, **43**, p 1238–1243
3. F.G. Caballero, R. Rementeria, L. Morales-Rivas, M. Benito-Alfonso, J.R. Yang, D. De Castro, J.D. Poplawsky, T. Sourmail, and C. Garcia-Mateo, Understanding Mechanical Properties of Nano-Grained Bainitic Steels from Multiscale Structural Analysis, *Metals*, 2019, **9**, p 426–434
4. A. Kumar and A. Singh, Mechanical properties of nanostructured bainitic steels, *Materialia*, 2021, **15**, 101034
5. H. Lan, L. Du, N. Zhou, and X. Liu, Effect of Austempering Route on Microstructural Characterization of Nanobainitic Steel, *Acta Metall. Sin. Engl. Lett.*, 2014, **27**, p 19–26
6. Y. Huang, A. Zhao, J. He, X. Wang, Z. Wang, and L. Qi, Microstructure, Crystallography and Nucleation Mechanism of NANOBAIN Steel, *Int. J. Miner. Metall.*, 2013, **20**, p 1155–1163
7. T. Sourmail, C. Garcia-Mateo, F.G. Caballero, L. Morales-Rivas, R. Rementeria, and M. Kuntz, Tensile Ductility of Nanostructured Bainitic Steels: Influence of Retained Austenite Stability, *Metals*, 2017, **7**, p 31–37
8. C.N. Hulme-Smith and H.K.D.H. Bhadeshia, Mechanical Properties of Thermally-Stable, Nanocrystalline Bainitic Steels, *Mater. Sci. Eng. A*, 2017, **700**, p 714–720
9. L. Morales-Rivas, C. Garcia-Mateo, T. Sourmail, M. Kuntz, R. Rementeria, and F.G. Caballero, Ductility of Nanostructured Bainite, *Metals*, 2016, **6**(12), p 302–321
10. H.K.D.H. Bhadeshia, Bulk Nanocrystalline Steel, *Ironmak. Steelmak.*, 2005, **32**, p 405–410
11. O. Ríos-Diez, R. Aristizábal-Sierra, C. Serna-Giraldo, J.A. Jimenez, and C. Garcia-Mateo, Development of Nanobainitic Microstructures in

Carbo-Austempered Cast Steels: Heat Treatment, Microstructure and Properties, *Metals*, 2020, **10**, p 635–652
12. C. Garcia-Mateo, G. Paul, M.C. Somani, D.A. Porter, L. Bracke, A. Latz, Garcia De Andres, and F.G. Caballero, Transferring Nanoscale Bainite Concept to Lower C Contents: A Perspective, *Metals*, 2017, **7**, p 159–172
13. H. Mousalou, S. Yazdani, N. Parvini Ahmadi, and B. Avishan, Nanostructured Carbide-Free Bainite Formation in Low Carbon Steel, *Acta Metall. Sin. Engl. Lett.*, 2020, **33**, p 1635–1644
14. H. Mousalou, S. Yazdani, B. Avishan, N. Parvini Ahmadi, A. Chabok, and Y. Pei, Microstructural and Mechanical Properties of Low-carbon Ultra-Fine Bainitic Steel Produced by Multi-Step Austempering Process, *Mater. Sci. Eng. A*, 2018, **734**, p 329–337
15. A. Eres-Castellanos, L. Morales-Rivas, A. Latz, F.G. Caballero, and C. Garcia-Mateo, Effect of Ausforming on the Anisotropy of Low Temperature Bainitic Transformation, *Mater. Charact.*, 2018, **145**, p 371–380
16. M. Zhang, Y. Wang, C. Zheng, F. Zhang, and T. Wang, Effects of Ausforming on Isothermal Bainite Transformation Behaviour and Microstructural Refinement in Medium-Carbon Si–Al-Rich Alloy Steel, *Mater. Des.*, 2014, **62**, p 168–174
17. V.G. Efremenko, O. Hesse, Th. Friedrich, M. Kunert, M.N. Brykov, K. Shimizu, V.I. Zurnadzhy, and P. Šuchmann, Two-Body Abrasion Resistance of High-Carbon High-Silicon Steel: Metastable Austenite vs Nanostructured Bainite, *Wear*, 2019, **418–419**, p 24–35
18. Y. Du, X. Wang, D. Zhang, X. Wang, C. Ju, and B. Jiang, A Superior Strength and Sliding Wear Resistance Combination of Ductile Iron with Nanobainitic Matrix, *J. Mater. Res. Technol.*, 2021, **11**, p 1175–1183
19. Z. Yang, F. Zhang, Nanostructured Bainitic Bearing Steel, *ISIJ Int.*, 2020, p. 18-30
20. K. Hayrynen, K. Brandenberg, and J. R. Keough, "Carbo-Austempering™-A New Wrinkle?" SAE Technical paper; SAE: Warrendale, PA, USA, 2002
21. O. Ríos-Diez, R. Aristizábal-Sierra, C. Serna-Giraldo, A. Eres-Castellanos, and C. Garcia-Mateo, Wear behavior of nanostructured carboaustempered cast steels under rolling-sliding conditions, *J. Mater. Res. Technol.*, 2021, **11**, p 1343–1355
22. H.K.D.H. Bhadeshia, Materials Algorithms Project, available at https://www.msm.cam.ac.uk/map/steel/programs/mucg83.html
23. L.C. Chang and H.K.D.H. Bhadeshia, Austenite Films in Bainitic Microstructures, *J. Mater. Sci. Technol.*, 1995, **11**, p 874–881
24. D.J. Dyson and B. Holmes, Effect of Alloying Additions on the Lattice Parameter of Austenite, *J. Iron Steel Ins.*, 1970, **208**, p 469–474
25. B.D. Cullity and S.R. Stock, *Elements of X-ray Diffraction*, 3rd ed. Prentice Hall, New York, 2001
26. J. Cornide, C. Garcia-Mateo, C. Capdevila, and F.G. Caballero, An Assessment of the Contributing Factors to the Nanoscale Structural Refinement of Advanced Bainitic Steels, *J. Alloys. Compd.*, 2013, **577**, p 43–47
27. J. Cornide, G. Miyamoto, F.G. Caballero, T. Furuhara, M.K. Miller, and C. Garcia-Mateo, Distribution of Dislocations in Nanostructured Bainite, *Solid State Phenom.*, 2011, **172**, p 117–122
28. F.G. Caballero, H.W. Yen, M.K. Miller, J.R. Yang, J. Cornide, and C. Garcia-Mateo, Complementary Use of Transmission Rlectron Microscopy and Atom Probe Tomography for the Examination of Plastic Accommodation in Nanocrystalline Bainitic Steels, *Acta Mater.*, 2011, **59**, p 6117–6123
29. B. Avishan, S. Yazdani, F.G. Caballero, T.S. Wang, and C. Garcia-Mateo, Characterisation of Microstructure and Mechanical Properties in Two Different Nanostructured Bainitic Steels, *Mater. Sci. Technol.*, 2015, **31**, p 1508–1520
30. H.K.D.H. Bhadeshia and A.R. Waugh, Bainite: An Atom-Probe Study of the Incomplete Reaction Phenomenon, *Acta Metall.*, 1982, **30**, p 775–784
31. C. Garcia-Mateo, F.G. Caballero, T. Sourmail, J. Cornide, V. Smanio, and R. Elvira, Composition Design of Nanocrystalline Bainitic Steels by Diffusionless Solid Reaction, *Met. Mater. Int.*, 2014, **20**, p 405–415
32. F.G. Caballero, M.K. Miller, C. Garcia-Mateo, and J. Cornide, New Experimental Evidence of the Diffusionless Transformation Nature of Bainite, *J. Alloys. Compd.*, 2013, **577**, p 626–630
33. S. Ahmadi Miab, B. Avishan, and S. Yazdani, Wear Resistance of Two Nanostructural Bainitic Steels With Different Amounts of Mn and Ni, *Acta Metall. Sin. Engl. Lett.*, 2016, **29**, p 587–594
34. A. Leiro, A. Kankanala, E. Vuorinen, and B. Prakash, Tribological Behaviour of Carbide-Free Bainitic Steel Under Dry Rolling/Sliding Conditions, *Wear*, 2011, **273**, p 2–8